Small Angle X-Ray Scattering from Lipid-Bound Myelin Basic Protein in Solution

H. Haas,*† C. L. P. Oliveira,† I. L. Torriani,†‡ E. Polverini,§ A. Fasano,¶ G. Carlone,¶ P. Cavatorta,§ and P. Riccio‖
*Universidade de São Paulo-Faculdade de Filosofia, Ciências e Letras de Ribeirão Preto, Ribeirão Preto, Brazil; †Instituto de Fisica, Laboratório de Cristalografia Aplicada e Raios X, Universidade Estadual de Campinas, Brazil; ‡Laboratório Nacional de Luz Síncrotron, Campinas, Brazil; §Dipartimento di Fisica and Istituto Nazionale per la Fisica della Materia, University of Parma, Parma, Italy; ¶Dipartimento di Biochimica e Biologia Molecolare, University of Bari, Bari, Italy; and ‖Dipartimento di Biologia, Difesa e Biotecnologie Agro-forestali, University of Basilicata, Potenza, Italy

ABSTRACT The structure of myelin basic protein (MBP), purified from the myelin sheath in both lipid-free (LF-MBP) and lipid-bound (LB-MBP) forms, was investigated in solution by small angle x-ray scattering. The water-soluble LF-MBP, extracted at pH < 3.0 from defatted brain, is the classical preparation of MBP, commonly regarded as an intrinsically unfolded protein. LB-MBP is a lipoprotein-detergent complex extracted from myelin with its native lipidic environment at pH > 7.0. Under all conditions, the scattering from the two protein forms was different, indicating different molecular shapes. For the LB-MBP, well-defined scattering curves were obtained, suggesting that the protein had a unique, compact (but not globular) structure. Furthermore, these data were compatible with earlier results from molecular modeling calculations on the MBP structure which have been refined by us. In contrast, the LF-MBP data were in accordance with the expected open-coil conformation. The results represent the first direct structural information from x-ray scattering measurements on MBP in its native lipidic environment in solution.

INTRODUCTION

The myelin sheath of the central nervous system is the lipid-rich, multilamellar membrane tightly wrapped around the nerve axon (Stoffel, 1990; Kirschner and Blaurock, 1992; Moscarello, 1996). Myelin basic protein (MBP) is the second major protein in myelin and perhaps the most studied among its components. MBP is important for two reasons: 1), it is believed to have the key role of biological ''glue'' for the formation, compaction, and maintenance of the multilamellar structure of myelin (Riccio et al., 1986; Readhead et al., 1987); and 2), it is a candidate autoantigen in the context of multiple sclerosis research, since it can induce Experimental Allergic Encephalomyelitis, an animal model of multiple sclerosis (Alvord et al., 1984; Massacesi et al., 1993). Up to the present time, besides the amino-acid sequence and the numerous posttranslational modifications, and a structural model of the 18.5 kDa isoform based in part on electron microscopical data (Beniac et al., 1997; Ridsdale et al., 1997), very little is known about the native three-dimensional protein conformation. One reason is that MBP is usually extracted under rather drastic conditions in a lipid-free, water-soluble form (LF-MBP), and at least partial unfolding must take place (Deibler et al., 1972, 1984). In fact, most studies on the structure of LF-MBP in aqueous solution are in agreement with a flexible coil conformation of the protein (Krigbaum and Hsu, 1975; Gow and Smith, 1989; Smith, 1992). However, the interaction of MBP with detergents, lipids, and other molecules can induce a more ordered structure (Smith, 1982; Haas et al., 1998; Polverini et al., 1999) and lipid-protein interactions are critical for the stability of the myelin sheath (Boggs et al., 1982; Smith, 1992; Staugaitis et al., 1996).

Another way to extract MBP from myelin is to use mild detergents, to maintain the protein in its natural lipidic environment during the purification process (Riccio et al., 1984, 1994). This form is called lipid-bound MBP (LB-MBP). LB-MBP was found to differ in various, mainly immunological, aspects from the lipid-free form (Bobba et al., 1991; Lolli et al., 1993; Massacesi et al., 1993; Liuzzi et al., 1996; Vergelli et al., 1997; Mazzanti et al., 1998). By spectroscopic measurements it was shown that LB-MBP has a much higher proportion of ordered secondary structure than the LF-MBP even after addition of detergents and lipids (Polverini et al., 1999). With LB-MBP and lipids, self-organization of stable, myelinlike membranes could be induced under conditions in which lipids alone remained poorly organized (Riccio et al., 1986, 2000). A comparison between LF-MBP and LB-MBP has been discussed (Riccio and Quagliariello, 1993).

In the present study, to get direct insight into the structures of the lipid-free and the lipid-bound protein forms, we have performed small angle x-ray scattering (SAXS) measurements on LF-MBP and LB-MBP solutions at the National Synchrotron Laboratory in Campinas, Brazil. The experimental data reveal considerable differences between the two protein forms. Moreover, we have modified the current structural model (Beniac et al., 1997; Ridsdale et al., 1997) taking into account circular dichroism (CD) results and theoretical predictions (Polverini et al., 1999). The x-ray scattering data on LB-MBP are in accordance with this new model.

MATERIALS AND METHODS

Protein purification

Lipid-free (LF) MBP

MBP was purified in the water-soluble, lipid-free form from bovine brain according to established procedures (Deibler et al., 1972, 1984). Protein

Submitted May 21, 2003, and accepted for publication September 9, 2003.
Address reprint requests to P. Riccio, E-mail: riccio@unibas.it.

0006-3495/04/01/455/06 $2.00

concentration was determined using the Bio-Rad Bradford reagent (Bio-Rad Laboratories, Hercules, CA) and a microassay procedure. MBP was used as a standard, using the molar extinction coefficient $\varepsilon = 10{,}300\ M^{-1}$ at 276.4 nm (Liebes et al., 1975).

Lipid-bound (LB) MBP

LB-MBP was purified as described previously. Briefly, highly purified myelin was treated with the zwitterionic detergent CHAPS (3-((3-cholamido-propyl)dimethylammonio)-1-propane sulfonate) (Boehringer Mannheim, Germany), hydroxyapatite (Bio-Rad Laboratories, Hercules, CA) was used as a filter to separate the nonadsorbed MBP from other myelin proteins, and overnight dialysis was used to remove free lipids from the LB-MBP complex. As the lipid-free counterpart, LB-MBP was electrophoretically pure. Protein purity was also assessed with the MALDI-TOF Pro mass spectrometer of Amersham Biosciences (Freiburg, Germany). Thin-layer chromatography (TLC) showed that the MBP was associated with all native myelin lipids. Relative percentages of lipids in LB-MBP, referred to the values obtained by computerized densitometry of HPTLC plates, were the following (in brackets are shown the percentages of lipids present in whole myelin): cholesterol, 31.5% (44.1%); nonhydroxycerebrosides, 2.5% (5.1%); hydroxycerebrosides, 6.0% (10.9%); sulphatides, 1.5% (7.6%); phosphatidylethanolamine 48.0% (12.8%); phosphatidylserine, 2.5% (3.3%); phosphatidylcholine, 7.0% (3.3%); and sphingomyelin, 1.0% (9.4%). Phosphatidylinositol (3.6% in native myelin) was not detectable in LB-MBP studied in this work.

Structural model of bovine MBP

The three-dimensional homology model of bovine MBP (18.5 kDa isoform) was based on the template of the human 18.5 kDa MBP structure (Ridsdale et al., 1997), using the coordinates available in the Protein Data Bank (Berman et al., 2000), entry ID code 1qcl. The pairwise alignment of human and bovine MBP was performed at the European Bioinformatics Institute using the BLAST network service (Altschul et al., 1997). Where required, single residue substitutions were performed using the tools available in the WHAT IF software (Vriend, 1990). Furthermore, the H10 and G11 residues of human MBP, which are not present in the bovine protein, were cut from the model, and the gap ends were joined with the paste tool in WHAT IF. The bovine Q75 was inserted into the structure and its side-chain conformations were generated using the rotamer library also included in WHAT IF. On the basis of a previous secondary structure prediction and the CD results of Polverini et al. (1999), the two coil segments of bovine MBP corresponding to residues 61–66 and 131–136 were replaced with two small α-helices, and energy-minimized by means of the Sybyl software package (SYBYL 6.7.1, Tripos, St. Louis, MO). The refined model was evaluated using the WHAT IF tools for protein structure verification.

X-ray scattering experiments

Small angle x-ray scattering experiments were performed at the SAXS beamline of the National Synchrotron Laboratory, Campinas, Brazil (Kellermann et al., 1997). The monochromatic beam was tuned at 7.711 keV. The experimental setup included a temperature-controlled, 1-mm-thick sample cell with thin (30-μm) mica windows and a linear position-sensitive detector. Two sample/detector distances were used, 1600 and 525 mm. Protein samples, containing buffer and detergent, were lyophilized and shipped at ambient temperature from Italy to Brazil. Directly before the x-ray scattering experiments, Milli-Q filtered water (Millipore, Bedford, MA) was added to the lyophilized samples to give the desired protein concentration, and these stock solutions were used directly. Blank (buffer) measurements were performed with solutions containing all the additives used for the protein measurements. The LB-MBP measurements were performed at a protein concentration of 1.28 mg/ml in 20 mM HEPES buffer, pH 7.5, with 0.8% CHAPS. The LF-MBP measurements were performed at a protein concentration of 3.2 mg/ml in 10 mM HEPES buffer, pH 7.5, with 0.4% CHAPS.

All solutions were agitated with a vortexer directly before the measurements. A volume of ~300 μl of solution was necessary for each experiment. The samples were kept at 15°C during the exposures. The time for a single measurement did not exceed 10 min, and the buffer (blank) measurements were performed immediately before or after the protein measurements. In some cases, several cycles of protein and buffer measurements were repeated, and the data were combined for better statistics. Data treatment was performed using the software package TRAT1D (Oliveira et al., 1997). Usual corrections for detector homogeneity, intensity of incident beam, sample absorption, and blank subtraction were included in this routine. The output of this software provides the corrected intensities and error values necessary for data analysis.

RESULTS AND DISCUSSION

Small angle x-ray scattering of LF-MBP and LB-MBP

The SAXS measurements from LB-MBP and LF-MBP are shown in Fig. 1. As can be seen already by qualitative inspection, the two data sets are clearly different. For LB-MBP, data with good signal/noise ratio were obtained showing a typical modulation of the scattering from globular particles. The Q-range detected was $0.02302 < Q < 0.2549$ Å^{-1}, where Q is the momentum transfer ($Q = 4\pi \sin(\theta)/\lambda$, where λ is the wavelength used and 2θ is the scattering

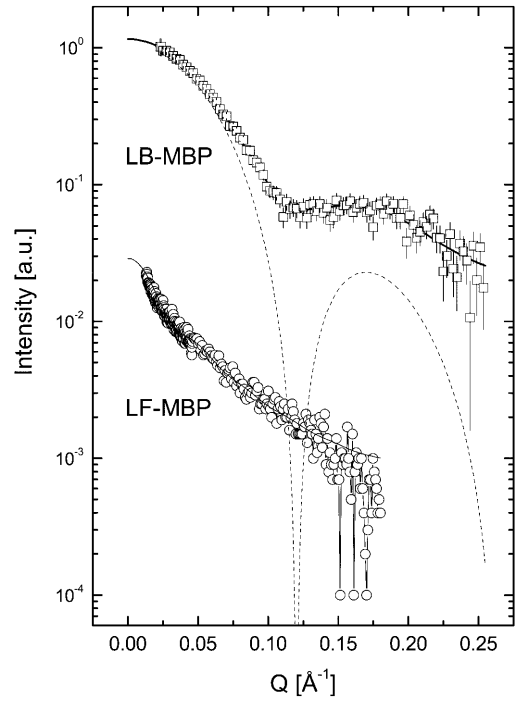

FIGURE 1 Small angle scattering from lipid-bound MBP (*upper data set*) and lipid-free MBP (*lower data set*). The LF-MBP data are divided by a factor of *xyz*. The solid lines were obtained from *xyz* data fitting (see text for details). The dotted line in the LB-MBP data set is the result from GNOM data fitting.

angle). In contrast, the LF-MBP curves did not show such a distinct modulation. The noise was much greater, and the scattering intensity reached zero at lower Q-values than with the LB-MBP.

The differences between the scattering curves become more apparent after analysis of the low Q-range by the so-called Guinier plot (Guinier and Fournet, 1955). In a plot of the logarithmic scattering intensity ln $I(Q)$ as a function of the square of the momentum transfer, Q, for monodisperse scatterers, the radius of gyration R_G is determined using

$$\ln I(Q) \propto -\frac{R_G^2 Q^2}{3}. \quad (1)$$

Fig. 2 shows the Guinier plot for the measurements on the two proteins. For the measurements of LB-MBP (*upper curve*), a straight line is obtained, indicating that, in fact, the protein existed in the solution in a unique, well-defined conformation. From linear regression in the range of Q^2 from 0.001 to 0.002 Å^{-2}, a value for R_G of 29.7 Å is obtained. The linear approximation is shown as a straight line, extrapolated for the whole Q^2-range.

For LF-MBP (*lower curve*), the data were less clear. First of all, the experimental noise was much higher, because of the lower scattering intensity. The slope is higher than in the previous case, and it is not constant over the total range of the measurement. Thus, no unique compact protein structure can be deduced from the data. The most unambiguous region is at the low Q^2 limit, ~0.0005 Å^{-2}. There, from linear regression (*solid line*), an R_G value in the order of 50 Å can be determined. At higher Q^2 (~0.0015 Å^{-2}), the slope is smaller, corresponding to an R_G of 42 Å. These results are, in some respects, similar to those obtained previously by SAXS of LF-MBP under somewhat different environmental conditions (without detergent), where radii of 46 Å (Krigbaum and Hsu, 1975), and of 39 Å (Epand et al., 1974) were determined. The present data indicate clearly that the conformation of LF-MBP is fundamentally different from that of LB-MBP.

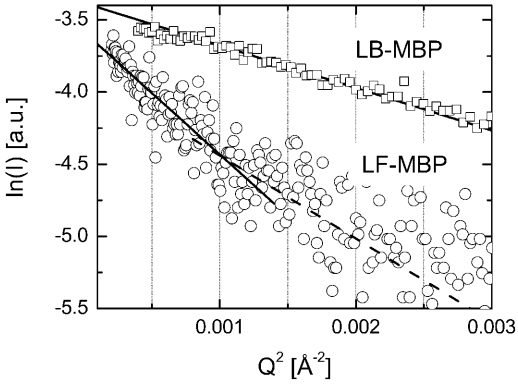

FIGURE 2 Guinier plot of the low Q-region for the LB-MBP and the LF-MBP measurements. For better comparison the LF-MBP data were vertically shifted. The straight lines were obtained from linear regression in the respective Q^2-regions.

Solution structure of LB-MBP

The main objective of the present research was to elucidate the solution structure of LB-MBP. Because the LB-MBP was present in the solution in a monodisperse, compact form, the data permitted further quantitative analysis. As a first step, the pair distribution function of the single protein molecule, $p(r)$ as given by

$$p(r) = 4\pi r^2 \int r'^2 \rho(r_1)\,\rho(r' + r)dr', \quad (2)$$

was calculated to get further information about the electron density distribution. Fig. 3 shows the function, calculated from the experimental data, $I(Q)$, using the software package GNOM (Semenyuk and Svergun, 1991) as

$$p(r) = \frac{1}{2\pi^2}\int I(Q)\,Qr\sin(Qr)dQ. \quad (3)$$

As can be seen, a maximum at ~40 Å and a shoulder at ~20 Å are visible. As well, the value at larger distances does not directly reach zero until beyond 100 Å. The data are in accordance with a compact protein conformation; however, the protein cannot have a homogeneous globular shape, because then a curve with a single maximum would be expected.

A shoulder in the $p(r)$ function, as found here, can be due to an arrangement of concentric spheres with different electron density, and, in fact, for the LB-MBP, it is expected that a shell of lipids or detergent is present around the protein. As a test, with the software package DECON (Glatter, 1981), the data for LB-MBP were fitted using such a model of concentric spheres, without any other restriction. The fit is shown in Fig. 1 as a dotted line for comparison with the experimental data. In Fig. 4, the curve for the real space model is shown. The electron density profile consists of 10 equidistant steps (shells) of constant electron density. It can be interpreted in terms of an inner sphere with a diameter in

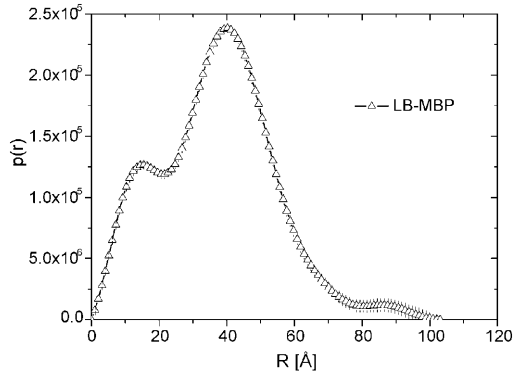

FIGURE 3 $P(r)$ for the LB-MBP measurement. See text for details.

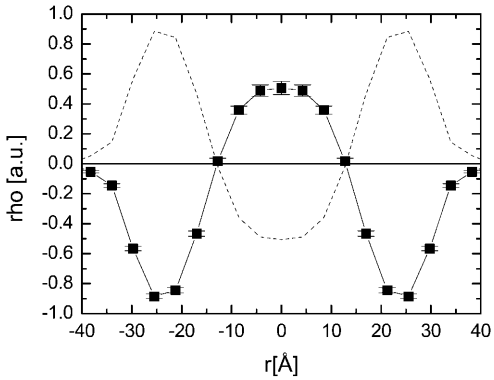

FIGURE 4 Electron density profile according to the GNOM fitting. As the sign of the profile cannot be determined, both curves—the one as shown by the solid line and the one as shown by the dotted line—correspond to the fit. The corresponding fit is shown as a dotted line in Fig. 1.

the order of 30 Å, where the electron density is higher than that of water, surrounded by a shell of ~15 Å thickness, with a density lower than that of water (a profile with inverted signs, such as shown by *dotted line* in Fig. 4, gives the same fit). Such a conformation could account for the expected organization of the protein (with high electron density), which is surrounded by a shell of lipids and detergent (with low electron density due to the hydrocarbon chains). As well, the dimensions roughly correspond to the expected values. For the protein, the volume can be estimated on the basis of the partial molar volumes of the amino acids (Perkins, 1988) to be 21,000 $Å^3$, corresponding to a compact sphere with a radius of 17 Å. Similarly, the dimension of the outer shell is as expected for a lipid envelope. With the present model, some aspects of the radial density distribution can be derived. However, with this formalism, only strictly centrosymmetric structures can be represented. The differences between the fit (*dotted line* in Fig. 1) and the experimental data are due to this limitation and they indicate that the protein structure significantly differs from such a centrosymmetric arrangement. To obtain more detailed information on the protein structure, further modeling is necessary.

Structural model of LB-MBP

To permit modeling of a complex three-dimensional protein shape, data fitting with another algorithm was performed. At a resolution of 5 Å, a protein structure can be considered as an assembly of so-called dummy residues centered at determined positions. A three-dimensional model of a protein can therefore be constructed from solution scattering data by finding a chain-compatible arrangement of the dummy residues that fits the experimental scattering pattern. The details on the program algorithm are given in Svergun et al. (2001). Thus, briefly stated, the protein is represented by an atomic structure composed of N residues. To represent the bounded solvent, the protein is surrounded by a hydration layer of 3 Å thickness, given by a quasiuniform grid of $M \approx N$ dummy solvent atoms placed 5 Å outside the protein. The scattering intensity from the chain model, composed of K atoms ($K = M + N$) averaged by all orientations can be calculated using the Debye formula,

$$I(q) = \sum_{i=1}^{K} \sum_{j=1}^{K} g_i(q) g_j(q) \frac{\sin(q r_{ij})}{q r_{ij}}, \qquad (4)$$

where g_i and g_j are the form factors for the dummy residue and solvent, respectively, and r_{ij} is the distance between the points i and j inside the protein. In the optimization procedure, an initial spherical arrangement of the chain model is constructed and the program searches for the best configuration of this model that minimizes the discrepancy between the experimental calculated scattered intensity using simulated annealing.

This approach has the advantage that it is model-free, and a very good agreement with the data can be achieved (*solid line* in Fig. 1). However, the spatial averaging of the protein orientation causes a dramatic loss of information in a SAXS profile. Also, we have access to just a small region of the reciprocal space and, as a result, a very large number of models can correspond to the same perfect fit. In Fig. 5 (*left panel*), the result of this model-free fitting is given. The results of five independent fittings, each drawn in a different color, are superimposed. Obviously, all results have some common features. The shapes have some anisotropy and they consist of a curved shape with some branches. The superposition gives the most probable configuration space available for the models as a hint about the possible shape of the protein. It should also be pointed out that in this model, no regions of different electron density can be considered. However, despite these restrictions, these shapes have some

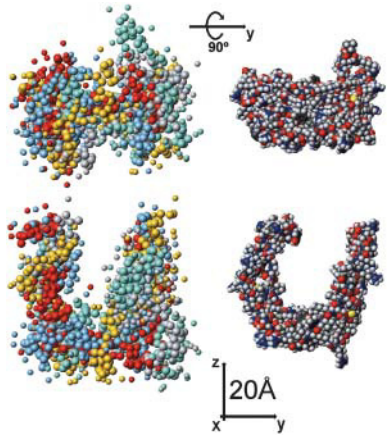

FIGURE 5 Comparison of the results from model-free data analysis (*left*) and from model calculations (*right*). The upper and the lower models show the protein in two different orientations. For the data analysis, five independent results from the fitting were superimposed. Each individual fit is shown by a different color. The molecular model is shown in the corresponding orientations.

striking similarities with results from previous model calculations, where an overall C-shape structure for the human MBP in the presence of lipids was built up using both experimental (electron microscopy) and computational techniques (Beniac et al., 1997; Ridsdale et al., 1997). Starting from this structure (entry 1qcl in Protein Data Bank) and using more recent CD results and refined theoretical predictive methods, a new model for MBP has been obtained. In fact, CD experiments carried out on LB- and LF-MBP (Polverini et al.,1999) clearly showed that the LB form appears to have a consistent amount of ordered secondary structure, while the LF-MBP is a substantially random coil protein. In the same article, theoretical predictions made using different computational methods were shown. These predictions confirmed the tendency of the LB protein to assume ordered secondary structure in accordance with the CD experiments. The main differences with respect to the 1qcl model are in the replacement of two coil segments (residues 61–66 and 131–136), which lie at the two ends of the C-shaped model with α-helical structures, although the characteristic C-shape is maintained. In Fig. 5, different orientations of this model (*right-hand side*) are shown in comparison with the result from the SAXS data analysis (*left-hand side*).

According to this qualitative inspection, the protein shape as given from the model calculations and the results from model-free SAXS data analysis are in good accordance. In fact, a C-shaped protein where water, lipid, and detergent molecules are inside, would account for the electron density gradient from DECON analysis (Fig. 4), bearing in mind that the curve with opposite signs (*dotted line*) corresponds equally well to the fit. For the evaluation of the possible protein structures to further detail, data analysis up to high Q-values is required. Therefore, with the present data sets, which for experimental reasons are limited in Q, the range of structures which are in accordance with the experimental data could be limited to a certain extent. For further refinement other measurements, where the detected Q-range is higher, will be necessary. This will allow also to validate detailed differences in model structures on the basis of experimental data.

CONCLUDING REMARKS

The fundamental aim of this work was to demonstrate the importance of studying MBP extracted and purified in its native lipidic environment when compared with the corresponding lipid-free form. In fact, a recent review reinforces our original idea that the isolation of specific protein-lipid complexes may be the more desirable goal for structural and functional studies of membrane proteins (Garavito and Ferguson-Miller, 2001), supposing they are structured and stable (Rosenbusch, 2001).

In this article, we have shown the first direct structural information about the conformation of MBP in solution in its native lipidic environment as obtained by small-angle x-ray scattering measurements. A fundamental outcome of this work is that MBP, extracted and purified in its lipidic environment by the procedure as proposed by us, appears suitable for studying the native protein structure and function. The direct isolation of the specific protein-lipid complex is more appropriate than trying to ''re-nature'' the lipid-free, denatured, protein variety by exposing it to a suitable environment. The data about the conformation of MBP in its native lipidic environment in solution point toward a compact, but not spherical, protein-lipid complex with regions of different electron density. Model-free fitting of the LB-MBP data yielded an extended C-shape for the protein, reminiscent of the predicted structure of the Protein Data Bank. From our further refinement we predict that the protein must be flattened (the *C* straightens out) in vivo within the major dense line of myelin, where it also interacts with other proteins and where the whole structure is more restrained (cf. Bates and Harauz, 2003). We conclude that even though LB-MBP is still a limited experimental construct, it represents a step in the right direction and an experimentally tractable model system for the natural protein in the myelin membrane.

Part of this article has been presented at the European Science Foundation Exploratory Workshop on ''Myelin Structure and Its Role in Autoimmunity,'' held in Potenza, Italy, 5–8 June 2002.

The major portion of the experimental work was performed at the National Synchrotron Light Laboratory, Brazil, and was sponsored by Coordenação de Aperfeiçoamento de Pessoal de Nível Superior, Brazil, Fundação de Amparo à Pesquisa do Estado de São Paulo (Proc.00/15087-4), Brazil, and Conselho Nacional de Pesquisa, Brazil. Funding from the European Union (Biomed contract BMH4-CT96-0990; Project title: High-Resolution Structures of Myelin Proteins), the Italian Foundation for Multiple Sclerosis, and Istituto Nazionale per la Fisica della Materia is also gratefully acknowledged.

REFERENCES

Altschul, S. F., T. L. Madden, A. A. Z. J. Schäffer, Z. Zhang, W. Miller, and L. D. J. Gapped. 1997. BLAST and PSI-BLAST: a new generation of protein database search programs. *Nucleic Acids Res.* 25:3389–3402.

Alvord, E. C., M. W. Kies, and A. L. Suckling. 1984. Experimental Allergic Encephalomyelitis: a useful model for Multiple Sclerosis. Alan R. Liss Inc., New York.

Bates, I. R., and G. Harauz. 2003. Molecular dynamics exposes α-helices in myelin basic protein. *J. Mol. Mod.*, published online 24 July 2003.

Beniac, D. R., M. D. Luckevich, G. J. Czarnota, T. A. Tompkins, R. A. Ridsdale, F. P. Ottensmeyer, M. A. Moscarello, and G. Harauz. 1997. Three-dimensional structure of myelin basic protein. I. Reconstruction via angular reconstitution of randomly oriented single particles. *J. Biol. Chem.* 272:4261–4268.

Berman, H. M., J. Westbrook, Z. Feng, G. Gilliland, T. N. Bhat, H. Weissig, I. N. Shindyalov, and P. E. Bourne. 2000. The Protein Data Bank. *Nucleic Acids Res.* 28:235–242.

Bobba, A., I. Munno, B. Greco, N. M. Pellegrino, P. Riccio, E. Jirillo, and E. Quagliariello. 1991. On the spontaneous adherence of myelin basic protein to T-lymphocytes. *Biochem. Biophys. Res. Commun.* 180:1125–1129.

Boggs, J. M., M. A. Moscarello, and D. Papahadiopolos. 1982. Structural organization of myelin—role of lipid-protein interactions determined in model systems. *In* Lipid-Protein Interactions, Vol. 2. P. C. Jost and O. H. Griffith, editors. Wiley & Sons, New York. 1–51.

Deibler, G., R. E. Martenson, and M. W. Kies. 1972. Large-scale preparation of myelin basic protein from central nervous tissue of several mammalian species. *Prep. Biochem.* 2:139–165.

Deibler, G. E., L. F. Boyd, and M. W. Kies. 1984. Proteolytic activity associated with purified myelin basic protein. *In* Experimental Allergic Encephalomyelitis: A Useful Model for Multiple Sclerosis. E. C. Alvord Jr., M. W. Kies, and A. J. Suckling, editors. Liss, New York. 249–256.

Epand, R. M., M. A. Moscarello, B. Zierenberg, and W. J. Vail. 1974. The folded conformation of the encephalogenic protein of the human brain. *Biochemistry.* 13:1264–1267.

Garavito, R. M., and S. Ferguson-Miller. 2001. Detergents as tools in membrane biochemistry. *J. Biol. Chem.* 276:32403–32406.

Glatter, O. 1981. Convolution square root of band-limited symmetrical functions and its applications to small-angle scattering data. *J. Appl. Crystallogr.* 14:101–108.

Gow, A., and R. Smith. 1989. The thermodynamically stable state of myelin basic protein in solution is a flexible coil. *Biochem. J.* 257:535–540.

Guinier, A., and G. Fournet. 1955. Small-Angle Scattering of X-Rays. Wiley & Sons, New York.

Haas, H., M. Torrielli, R. Steitz, P. Cavatorta, R. Sorbi, P. Riccio, and A. Gliozzi. 1998. Myelin model membranes on solid substrate. *Thin Sol. Films.* 327–329:627–631.

Kellermann, G., E. Vicentin, E. Tamura, M. Rocha, H. Tolentino, A. Barbosa, A. Craievich, and I. Torriani. 1997. The small-angle x-ray scattering beamline of the Brazilian Synchrotron Light Laboratory. *J. Appl. Crystallogr.* 30:880–883.

Kirschner, D. A., and A. E. Blaurock. 1992. Organization, phylogenetic variations and dynamic transitions of myelin. *In* Myelin: Biology and Chemistry. R. E. Martenson, editor. CRC Press, Boca Raton, FL. 3–78.

Krigbaum, W. R., and T. S. Hsu. 1975. Molecular conformation of bovine A1 basic protein, a coiling macromolecule in aqueous solution. *Biochemistry.* 14: 2542–2546.

Liebes, L. F., R. Zand, and W. D. Phillips. 1975. Solution behavior, circular dichroism and 22 MHz PMR studies of the bovine myelin basic protein. *Biochim. Biophys. Acta.* 405:27–39.

Liuzzi, G. M., R. Tamborra, A. Ventola, F. Bisaccia, E. Quagliariello, and P. Riccio. 1996. Different recognition by clostripain of myelin basic protein in the lipid-bound and lipid-free forms. *Biochem. Biophys. Res. Commun.* 226:566–571.

Lolli, F., G. M. Liuzzi, M. Vergelli, L. Massacesi, C. Ballerini, L. Amaducci, and P. Riccio. 1993. Antibodies specific for the lipid-bound form of myelin basic protein during experimental autoimmune encephalomyelitis. *J. Neuroimmunol.* 44:69–76.

Massacesi, L., M. Vergelli, B. Zehetbauer, G. M. Liuzzi, J. Olivotto, C. Ballerini, A. Uccelli, L. Mancardi, P. Riccio, and L. Amaducci. 1993. Induction of the autoimmune encephalomyelitis in rats and immune response to myelin basic protein in lipid bound form. *J. Neurol. Sci.* 119:91–98.

Mazzanti, B., M. Vergelli, P. Riccio, R. Martin, H. F. McFarland, M. G. Liuzzi, L. Amaducci, and L. Massacesi. 1998. T-cell response to myelin basic protein and lipid-bound myelin basic protein in patients with Multiple Sclerosis and health donors. *J. Neuroimmunol.* 82:96–100.

Moscarello, M. A. 1996. Evolving biological concepts and therapeutic approaches. *In* Cell Biology and Pathology of Myelin. R. M. Devon, R. Doucette, B. H. J. Juurlink, A. J. Nazarali, D. J. Schreyer, and V. M. K. Verge, editors. Plenum Publishing, New York.

Oliveira, C. L. P., D. R. dos Santos, G. Kellermann, T. Plivelic, and I. L. Torriani. 1997. Data treatment program for the SAXS beamline. *LNLS Technical Note* (unpublished, available for beam line users).

Perkins, J. P. 1988. X-ray and neutron solution scattering. *In* Modern Physical Methods in Biochemistry, Part B. A. Neuberger and L. L. M. van Deenen, editors. Elsevier, Amsterdam, The Netherlands. 134–265.

Polverini, E., A. Fasano, F. Zito, P. Riccio, and P. Cavatorta. 1999. Conformation of bovine myelin basic protein purified with bound lipids. *Eur. Biophys. J.* 28:351–355.

Readhead, C., B. Popko, N. Takahashi, H. D. Shine, R. A. Saavedra, R. L. Sidman, and L. Hood. 1987. Expression of a myelin basic protein gene in transgenic mice: correlation of the dismyelinating phenotype. *Cell.* 48:703–712.

Riccio, P., J. P. Rosenbusch, and E. Quagliarello. 1984. A new procedure to isolate brain myelin basic protein in a lipid-bound form. *FEBS Lett.* 177:236–240.

Riccio, P., L. Masotti, P. Cavatorta, A. De Santis, D. Juretic, A. Bobba, I. Pasquali-Ronchetti, and E. Quagliariello. 1986. Myelin basic protein ability to organize lipid bilayers: structural transitions in bilayers of lysophosphatidylcholine micelles. *Biochem. Biophys. Res. Commun.* 134:313–319.

Riccio, P., and E. Quagliariello. 1993. Lipid-bound, native-like, myelin basic protein: a well-known protein in a new guise, or an unlikely story? *J. Neurochem.* 61:787–788.

Riccio, P., A. Bobba, E. Romito, M. Minetola, and E. Quagliariello. 1994. A new detergent to purify CNS myelin basic protein isoforms in lipid-bound form. *Neuroreport.* 24:689–692.

Riccio, P., A. Fasano, N. Borenshtein, T. Bleve-Zacheo, and D. A. Kirschner. 2000. Multilamellar packing of myelin modeled by lipid-bound MBP. *J. Neurosci. Res.* 59:513–521.

Ridsdale, R. A., D. R. Beniac, T. A. Tompkins, M. A. Moscarello, and G. Harauz. 1997. Three-dimensional structure of myelin basic protein. II. Molecular modeling and considerations of predicted structures in multiple sclerosis. *J. Biol. Chem.* 272:4269–4275.

Rosenbusch, J. P. 2001. Stability of membrane proteins: relevance for the selection of appropriate methods for high-resolution structure determinations. *J. Struct. Biol.* 136:144–157.

Semenyuk, V., and D. I. Svergun. 1991. GNOM—a program package for small angle scattering data processing. *J. Appl. Crystallogr.* 24:537–540.

Smith, R. 1982. Self-association of myelin basic protein: enhancement by detergents and lipids. *Biochemistry.* 12:2697–2701.

Smith, R. 1992. The basic protein of CNS myelin: its structure and ligand binding. *J. Neurochem.* 59:1589–1608.

Staugaitis, S. M., D. R. Colman, and L. Pedraza. 1996. Membrane adhesion and other functions for the myelin basic proteins. *Bioessays.* 18:13–18.

Stoffel, W. 1990. The myelin membrane of the central nervous system—essential macromolecular structure and function. *Angew. Chem. Int. Ed. Engl.* 29:958–976.

Svergun, D. I., M. V. Petoukhov, and M. H. J. Koch. 2001. Determination of domain structure of proteins from x-ray solution scattering. *Biophys. J.* 80:2946–2953.

Vergelli, M., V. Pinet, A. B. Vogt, M. Kalbus, M. Malnati, P. Riccio, E. O. Long, and R. Martin. 1997. HLA-DR-restricted presentation of purified myelin basic protein is independent of intracellular processing. *Eur. J. Immunol.* 27:941–951.

Vriend, G. 1990. WHAT IF: a molecular modeling and drug design program. *J. Mol. Graph.* 8:52–56.